

See discussions, stats, and author profiles for this publication at: <https://www.researchgate.net/publication/23234927>

Huang HP, Shih YW, Chang YC, Hung CN,  
Wang CJ.. Chemoinhibitory effect of mulberry  
anthocyanins on melanoma metastasis  
involved in the Ras/PI3K pathway. J Agric Food  
Chem 56: 9286–...

ARTICLE *in* JOURNAL OF AGRICULTURAL AND FOOD CHEMISTRY · SEPTEMBER 2008

Impact Factor: 2.91 · DOI: 10.1021/jf8013102 · Source: PubMed

---

CITATIONS

51

READS

34

---

5 AUTHORS, INCLUDING:



Hui-Pei Huang

Chung Shan Medical University

26 PUBLICATIONS 365 CITATIONS

[SEE PROFILE](#)



Chau-Jong Wang

Chung Shan Medical University

216 PUBLICATIONS 5,851 CITATIONS

[SEE PROFILE](#)

## Chemoinhibitory Effect of Mulberry Anthocyanins on Melanoma Metastasis Involved in the Ras/PI3K Pathway

HUI-PEI HUANG,<sup>†</sup> YUAN-WEI SHIH,<sup>§,†</sup> YUN-CHING CHANG,<sup>†</sup> CHI-NAN HUNG,<sup>‡</sup>  
AND CHAU-JONG WANG<sup>\*,†</sup>

Institute of Biochemistry and Biotechnology, Chung Shan Medical University, No. 110, Section 1,  
Chien-Kauo N. Road, Taichung 402, Taiwan, ROC, Department of Biological Science and  
Technology, Chung Hwa University of Medical Technology, No. 89, Wen-Hwa first Street, Jen-Te,  
Tainan 717, Taiwan, ROC, and Department of Holistic Wellness, Ming Dao University,  
No. 369, Wen-Hua Road, Peetow, ChangHua 523, Taiwan, ROC

Anthocyanins richly exist in mulberry plants and have been well characterized to have various bioactive properties. However, the antimetastasis properties of mulberry anthocyanins (MACs) remain unclear. The objectives of this study were to investigate the inhibitory effects of MACs on the metastasis of B16-F1 cells under noncytotoxic concentrations. Further investigation revealed that the antimetastatic effect of MACs was also evident in a C57BL/6 mice model. First, MACs exhibited an inhibitory effect on the migration ability by wound healing assay and Boyden chamber assay. In the cancer cell metastasis process, matrix degrading proteinases are required. B16-F1 cells treated with MACs at various concentrations showed reduced extracellular matrix (ECM) proteinases including matrix metalloproteinase-2 (MMP-2) and matrix metalloproteinase-9 (MMP-9) by gelatin zymography assay. The results of the Western blotting assay demonstrated that the expression levels of Ras, phosphoinositide 3-kinase (PI3K), phospho-Akt, and nuclear factor kappa B (NF- $\kappa$ B) in the MACs-treated B16-F1 cells were reduced. Therefore, it was suggested that MACs could mediate B16-F1 cell metastasis by reduction of MMP-2 and MMP-9 activities involving the suppression of the Ras/PI3K signaling pathway. Besides, B16-F1 melanoma cells were also injected into the right groin of the C57BL/6 mice, and the mice were fed with MACs at the same time. The hematoxylin-eosin stain (H&E stain) and immunohistochemistry stain showed that the MACs inhibited the metastasis of B16-F1 cells *in vivo*. Taken together, the findings proved the inhibitory effect of MACs on the growth and metastasis of B16-F1 cells. These results indicated that MACs might be offered for future application as an antimetastatic agent.

**KEYWORDS:** Mulberry anthocyanins; metastasis; migration; MMP-2; MMP-9; PI3K/Akt; NF- $\kappa$ B

### INTRODUCTION

Mulberry, the fruit of *Morus alba* L., is a traditional Chinese edible fruit that is used effectively in folk medicines for antibacterial, antibiotic, anti-inflammatory, antioxidative, and immune system-stimulating properties (1). Mulberry extracts contain high amounts of anthocyanins, which are the largest group of water-soluble pigments in the plant kingdom. They represent one of the most widely distributed classes of flavonoids in plants. Apart from their coloring effects in fruits, anthocyanins have been reported to have antitumor effects *in vitro* and *in vivo* (2). The common aglycon forms, anthocyanidins, found

are cyanidin, delphinidin, peonidin, petunidin, malvidin, and pelargonidin. They all have the basic flavylium cationic structure at low pH, and they differ from each other by having different substituents in ring B. This structure provides them with the bright red, orange, and blue colors (3).

Melanoma is a skin cancer that originates in melanocytes, specialized pigment-producing cells found in both the basal layer of the epidermis and in the eye (4). The known environmental risk factor is exposure to ultraviolet light, and the risk is greatly increased in people with fair skin (5). Normally, melanocytes synthesize melanin pigments and transfer them to surrounding keratinocytes. The resulting skin pigmentation protects against damage caused by solar ultraviolet radiation (6). Most diagnosed patients with lung melanoma are in an advanced stage because of its highly metastatic properties, and such patients are not candidates for surgical resection.

\* Corresponding author. Phone: +886 4 24730022 ext. 11670. Fax: +886 4 23248167. E-mail: wcj@csmu.edu.tw.

<sup>†</sup> Chung Shan Medical University.

<sup>§</sup> Chung Hwa University of Medical Technology.

<sup>‡</sup> Ming Dao University.

The metastasis is a multistep process involving an overexpression of proteolytic enzymes, such as MMP family, MMP-2, and MMP-9 (also known as type IV collagenases or gelatinases), which are capable of degrading most ECM components that form the basal membrane. Therefore, these two gelatinases are essential for tumor cell migration, tumor spreading, tissue invasion of tumor cells, and metastasis (7). Gelatinases (MMP-2 and MMP-9) are the major proteases in lung cancer and are closely correlated with invasive and metastatic potentials (8).

As well as MMPs, the extracellular signal regulating kinase (ERK) is also known to mediate metastasis. The ERK is activated by numerous extracellular stimuli and is involved in signal transduction cascades that play an important regulatory role in cell growth, differentiation, apoptosis, and metastasis (9, 10). In addition, the PI3K signal transduction pathway regulates cell metastasis of melanoma and is closely associated with the development and progress of various tumors (11). Therefore, the PI3K/Akt pathway is constitutively active in most tumors. In addition to its role in tumor cell invasion, this pathway also regulates many cellular processes implicated in tumorigenesis, cell size/growth, proliferation, survival, glucose metabolism, genome stability, metastasis, and angiogenesis (12).

Moreover, MMP gene expression is chiefly regulated by transcriptional factors (for example, NF- $\kappa$ B and AP-1) via the PI3K/Akt or ERK pathways (13, 14). NF- $\kappa$ B is a multisubunit transcription factor involved in cellular responses to viral infection and inflammation. The active NF- $\kappa$ B consists of a dimer of a Rel family/p65 subunit and a p50 or p52 subunit. NF- $\kappa$ B is maintained in the cytoplasm through interactions with an inhibitor of NF- $\kappa$ B (I $\kappa$ B), but upon dissociation, moves into the nucleus and promotes cancer cell proliferation, angiogenesis, and metastasis. c-Fos and c-jun also are important transcription factors and oncogenes, which form a heterodimer (AP-1 complex). It is associated with invasion and metastasis of cancer cells (15).

Ras-homologous (Rho) GTPases play a pivotal role in the regulation of numerous cellular functions associated with malignant transformation and metastasis. Members of the Rho family of small GTPases are key regulators of actin reorganization, cell motility, cell–cell and cell–extracellular matrix (ECM) adhesion as well as of cell cycle progression, gene expression, and apoptosis (16). RhoB shares 86% amino acid sequence identity with RhoA, yet the roles of the low-molecular-weight GDP/GTP binding GTPases in oncogenesis are quite different. While RhoA, like other GTPase family members such as Ras, Rac1, and Cdc42, promotes oncogenesis, invasion, and metastasis (17), emerging evidence points to a tumor-suppressive role for RhoB (18).

However, these studies on functions of anthocyanins have been mainly focused on the effects of inhibition of tumor cell metastasis, whereas the precise effect and related molecular mechanism of mulberry anthocyanins on melanoma metastasis was still unclear. Since cancer metastasis is highly related to degradation of extracellular matrix and cellular motility, the objective of this work was to examine the inhibitory effects and the related signaling pathways of mulberry anthocyanins on the metastasis of murine melanoma B16-F1 cells *in vitro* and *in vivo*.

## MATERIALS AND METHODS

**Materials.** DMSO, Tris-base, EDTA, SDS, phenylmethylsulfonyl fluoride, bovine serum albumin (BSA), leupeptin, Nonidet P-40, deoxycholic acid, and sodium orthovanadate were purchased from Sigma-Aldrich (St. Louis, MO). Phosphate buffer solution (PBS), trypsin-EDTA, and powdered Dulbecco's modified Eagle's medium

(DMEM) were purchased from Gibco/BRL (Gaithersburg, MD). Matrigel was from BD Biosciences (Bedford, MA). Antibody against Akt and MAPK/ERK1/2, phosphorylated proteins were purchased from Cell Signaling Tech. (Beverly, MA). PI3K (p85), NF- $\kappa$ B (p65), Ras, RhoA, and RhoB antibodies were from BD Transduction Laboratories (San Diego, CA).

**Plant.** Mulberry (fruit of *Morus alba* L.) was obtained from the Taichung District Agricultural Research Station in Tai-Pin, Taichung, Taiwan.

**Preparation of Mulberry Anthocyanins.** MACs were prepared from the lyophilized fruit of mulberry (100 g), with a 3-fold volume of methanol containing 1% HCl for 1 day at 4 °C. The extract was filtered and then concentrated under reduced pressure at 30 °C. The precipitate was collected and stood on an Amberlite Diaion HP-20 resin column for 24 h, then was cleaned in distilled water (5 L) containing 0.1% HCl solution and eluted with methanol. The filtrate was collected and lyophilized to obtain 5 g of MACs and stored at 4 °C before use (19).

**HPLC Assay for MACs.** Total anthocyanins were extracted using the Fuleki and Francis method (20). Separation of anthocyanins was conducted on a Luna C18(2) column (2.00 mm × 150 mm, 3.0  $\mu$ m, Phenomenex, Inc., Torrance, CA) using an HPLC system consisting of a Finnigan Surveyor module separation system and a photodiode-array (PDA) detector (Thermo Electron Co., MA, USA.) A linear gradient from 98% A to 30% B in 45 min was used for the HPLC analysis of anthocyanins. Solvent A was water containing 1% formic acid, and solvent B was acetonitrile containing 0.1% formic acid. The flow rate was 0.2 mL/min. Absorption spectra of anthocyanins were recorded from 240 to 600 nm with the in-line PDA detector.

**Cell Line and Cell Culture.** B16-F1, a murine melanoma cell line, was obtained from BCRC (Food Industry Research and Development Institute in Hsin-Chu, Taiwan). Cells were cultured in DMEM supplemented with 10% fetal calf serum, 2 mM L-glutamine, 100 U/mL penicillin and 100 mg/mL streptomycin mixed antibiotics, and 1 mM sodium pyruvate. All cell cultures were maintained at 37 °C in a humidified atmosphere of 5% CO<sub>2</sub>–95% air.

**Analysis of Cell Viability (MTT Assay).** To evaluate the cytotoxicity of MACs, MTT [3-(4,5-dimethylthiazol-2-yl)-2,5-diphenyltetrazolium bromide] assay was performed to determine cell viability. Briefly, cells were seeded at a density of  $1 \times 10^5$  cells/mL in a 24-well plate for 24 h. Then, the cells were treated with MACs at various concentrations (0, 1, 2, 3, 4, and 5 mg/mL) for various periods of time (1 day, 2 days, and 3 days). Afterward, the medium was changed and incubated with MTT solution (5 mg/mL)/well for 4 h. The medium was removed, and formazan was solubilized in isopropanol and measured spectrophotometrically at 563 nm.

**Analysis of MMP-2/MMP-9 Activity (Gelatin Zymography).** The activities of MMP-2 and MMP-9 were assayed by gelatin zymography as described previously (21). Briefly, samples were mixed with loading buffer and were electrophoresed on 8% SDS–polyacrylamide gel containing 0.1% gelatin at 140 V for 3 h. The gel was then washed twice in Zymography washing buffer (2.5% Triton X-100 in double-distilled H<sub>2</sub>O) at room temperature to remove SDS. Following incubation at 37 °C for 12–16 h in Zymography reaction buffer (40 mM Tris-HCl (pH 8.0), 10 mM CaCl<sub>2</sub>, and 0.02% Na<sub>3</sub>N), the gel was stained with Coomassie blue R-250 (0.125% Coomassie blue R-250, 0.1% amino black, 50% methanol, and 10% acetic acid) for 1 h and destained with methanol/acetic acid/water (20/10/70, v/v/v).

**Wound-Healing Assay.** To determine the cell motility, B16-F1 cells ( $1 \times 10^5$  cells /mL) were plated in 6-well culture plates and grown to 80–90% confluence. After aspirating the medium, in the center of the cell monolayer was scraped with a sterile micropipette tip to create a denuded zone (gap) of constant width. Subsequently, cellular debris was washed with PBS, then B16-F1 cells were exposed to various concentrations of MACs (0, 1, 2, and 3 mg/mL). Wound closure was monitored and photographed at 0, 1, 2, and 3 days by an Olympus CK-2 inverted microscope and an Olympus OM-1 camera. The migrated cells across the white lines were counted in five random fields from each triplicate treatment, and data are presented as the mean  $\pm$  SD.

**Boyden Chamber Migration Assay.** The migration abilities of the B16-F1 cells that were untreated or treated with various concentrations

of MACs were evaluated. After treatment for 24 h, cells were detached by trypsin and resuspended in serum-free medium. Medium containing 10% FBS was applied to the lower chamber as chemoattractant, and then cells were seeded on the upper chamber with 8  $\mu\text{m}$  pore polycarbonate filters at a density of  $1 \times 10^5$  cells/well in 50  $\mu\text{L}$  of serum-free medium. The chamber was incubated for 5 h at 37 °C. At the end of incubation, the cells that migrated to the lower surface of the membrane were fixed with methanol and stained with 5% Giemsa solution, and the cells in the upper surface of the membrane were carefully removed with a cotton swab. The migrating cells on the lower surface of the membrane filter were counted with a light microscope.

**Preparation of Whole-Cell Lysates and Nuclear Extracts.** The cells were lysed with iced-cold RIPA buffer (1% NP-40, 50 mM Tris-base, 0.1% SDS, 0.5% deoxycholic acid, and 150 mM NaCl, pH 7.5), and phenylmethylsulfonyl fluoride (10 mg/mL), leupeptin (17 mg/mL), and sodium orthovanadate (10 mg/mL) were freshly added. After vortexing for 30 min on ice, the samples were centrifuged at  $12,000 \times g$  for 10 min, and then the supernatants were collected as whole-cell lysates. The lysates were denatured, subjected to SDS-PAGE and Western blotting. Nuclear extracts were prepared as previously described (22) and then used for NF- $\kappa$ B and AP-1 detection. The nuclear pellet was resuspended in nuclear extract buffer (1.5 mM MgCl<sub>2</sub>, 10 mM HEPES, pH 7.9, 0.1 mM EDTA, 0.5 mM dithiothreitol, 0.5 mM phenylmethylsulfonyl fluoride, 25% glycerol, and 420 mM NaCl). The nuclear suspension was incubated on ice for 20 min and then centrifuged at  $14,000 \times g$  for 5 min. The supernatant (corresponding to the soluble nuclear fraction) was saved, and the remaining pellet was solubilized by sonication in PBS. The protein content was determined with Bio-Rad protein assay reagent using bovine serum albumin as a standard.

**Western Blotting Analysis.** To analyze the migration-related proteins, Western blotting was performed as follows. Whole-cell lysates (50  $\mu\text{g}$  purified protein) were mixed with a 5× sample buffer and boiled for 10 min. Then an equal protein content of total cell lysate from control and MAC-treated samples were resolved on 10–12% SDS-PAGE gels. Proteins were then transferred onto nitrocellulose membranes (Millipore, Bedford, MA) by electroblotting using an electroblotting apparatus (Bio-Rad). Nonspecific binding of the membranes was blocked with Tris-buffered saline (TBS) containing 1% (w/v) nonfat dry milk and 0.1% (v/v) Tween-20 (TBST) for more than 2 h. Membranes were washed with TBST three times for 10 min and incubated with appropriate dilution of specific primary antibodies in TBST overnight at 4 °C. Subsequently, the membranes were washed with TBST and incubated with an appropriate secondary antibody (horseradish peroxidase-conjugated goat antimouse or antirabbit IgG) for 1 h. After washing the membrane three times for 10 min in TBST, band detection was revealed by enhanced chemiluminescence using ECL Western blotting detection reagents and exposed ECL hyperfilm in FUJIFILM Las-3000 (Tokyo, Japan). Then proteins were quantitatively determined by densitometry using FUJIFILM-Multi Gauge V2.2 software.

**NF- $\kappa$ B and AP-1 Binding Assay.** Cell nuclear proteins were extracted by nuclear extract buffer and measured by electrophoretic mobility shift assay (EMSA). Cells ( $1 \times 10^5/\text{mL}$ ) were collected in PBS buffer (pH 7.4) and centrifuged at  $2000 \times g$  for 5 min at 4 °C. Cells were lysed with buffer A (10 mM HEPES, 1.5 mM MgCl<sub>2</sub>, 10 mM KCl, 0.5 mM DTT, and 0.5 mM PMSF (pH 7.9) containing 5% NP-40) for 10 min on ice, and this was followed by vortexing to shear the cytoplasmic membranes. The lysates were centrifuged at  $2000 \times g$  for 10 min at 4 °C. The pellet containing the nuclei was extracted with high salt buffer B (20 mM HEPES, 420 mM NaCl, 1.5 mM MgCl<sub>2</sub>, 0.5 mM DTT, 0.5 mM PMSF, 0.2 mM EDTA, and 25% glycerol) for 15 min on ice. The lysates were clarified by centrifuging at  $13,000 \times g$  for 10 min at 4 °C. The supernatant containing the nuclear proteins was collected and frozen at -80 °C until use.

Five microgram aliquots of nuclear proteins were mixed with either biotin-labeled NF- $\kappa$ B or AP-1 oligonucleotide probes for 15 min at room temperature. Oligonucleotides contained sense of NF- $\kappa$ B, 5'-AGTTGAGGGGACTTCCAGGC-3', antisense of NF- $\kappa$ B, 3'-TCAACTCCCCCT GAAAGGGTCCG-5'; sense of AP-1, 5'-

CGCTTGATGAGTGAGCCGGAA-3'; and antisense of AP-1, 3'-GCGAACTACTCAGTCGGCCTT-5'. DNA probes were added into a microcentrifuge tube with 20  $\mu\text{L}$  binding reactions containing double-distilled H<sub>2</sub>O, 5  $\mu\text{g}$  of nuclear protein, 1  $\mu\text{L}$  of poly-L-lysine, 1  $\mu\text{L}$  of poly (dI-dC), 2  $\mu\text{L}$  of biotin-labeled double-stranded NF- $\kappa$ B oligonucleotides, and 2  $\mu\text{L}$  of 10-fold binding buffer and were incubated for 15 min at room temperature. Specific competition binding assays were performed by adding 200-fold excess of unlabeled probe as a specific competitor. Following protein-DNA complex formation, samples were loaded on a 10% nondenaturing polyacrylamide gel in 0.5× TBE buffer and were then transferred to positively charged nitrocellulose membranes by a transfer blotting apparatus and cross-linked in a Stratagene cross-linker. Gel shifts were visualized with streptavidin-horseradish peroxidase followed by chemiluminescent detection.

**Measurement of Tumor Metastasis in Vivo.** To establish tumor metastasis, C57BL/6 mice (male, ~20 g, 6 weeks old) were purchased from the National Taiwan University Animal Center, Taiwan. Mice were randomly selected to be placed in one of six treatment groups (seven in each group) and were received by oral gavage. Group A mice (control) received 100  $\mu\text{L}$  of PBS three times per week. Group B was fed 3% MACs. Groups C–F were implanted with  $2 \times 10^6$  B16-F1 tumor cells suspended in 200  $\mu\text{L}$  of sterile PBS via a right inguinal injection. After 3 days, mice were fed by an oral gavage with 100  $\mu\text{L}$  of PBS (group C), 1% MAC (group D), 2% MAC (group E), and 3% MAC (group F) three times per week. During the 5 week feeding period, all mice used were handled according to the guidelines of the Instituted Animal Care and Use Committee of Chung Shan Medical University (IACUC, CSMC) for the care and use of laboratory animals. Mice were housed with a regular 12 h light/12 h dark cycle. After 35 days, mice were sacrificed for the assay of cell physiology (e.g., H&E stain and immunohistochemistry stain) and metastasis-related proteins (e.g., Western blotting).

**Statistical Analysis.** Data were expressed as the means  $\pm$  standard deviation of three independent experiments and were analyzed by Student's *t*-test (SigmaPlot 2001). Significant differences were established at  $p \leq 0.05$ .

## RESULTS

**Morus alba L. Anthocyanin Identification.** *Morus alba* L. (100 g) was extracted with distilled water and methanol as described in Materials and Methods to produce approximately 5 g of water-soluble dry powder (MACs). Spectrophotometer analysis of MACs showed that the purity of MACs was approximately 85–95% (20). As shown in our previous study, HPLC analysis of the identified anthocyanic compounds via LC-ESI/MS/MS revealed that the retention times of cyanidine-3-glucoside, cyanidine-3-rutinoside, pelargonidin-3-glucoside, and pelargonidin-3-rutinoside were 24.9, 25.8, 26.9, and 27.7 min, respectively. The data confirmed that cyanidin and pelargonidin are two major components in *Morus alba* L. anthocyanin.

**Cytotoxicity of MACs in B16-F1 cells.** Cell viability was assayed in cultures exposed to 1–5 mg/mL MACs for 1 day, 2 days, and 3 days. MACs showed dose- and time-dependent inhibitory effect on the growth of B16-F1 cells (Figure 1). B16-F1 were incubated with 1–5 mg/mL MACs for 1 day and 3 days, and the concentration of MACs inhibiting 50% of B16-F1 cell viability (IC<sub>50</sub>) was around 3.1 mg/mL and 2.5 mg/mL (Figure 1). After treatment with MACs (4.0 mg/mL) for 1 day and 3 days, approximately 77.5% and 100% of cell numbers were decreased, respectively. These results demonstrated that the treatment of MACs with doses higher than 4 mg/mL for 1 day, 2 days, and 3 days resulted in dose- and time-dependent loss of cell viability in B16-F1 cells, but doses lower than 3 mg/mL for 1 day, 2 days, and 3 days did not cause cytotoxicity. In the following experiments, these doses below 3 mg/mL for 1 day of MACs were used.

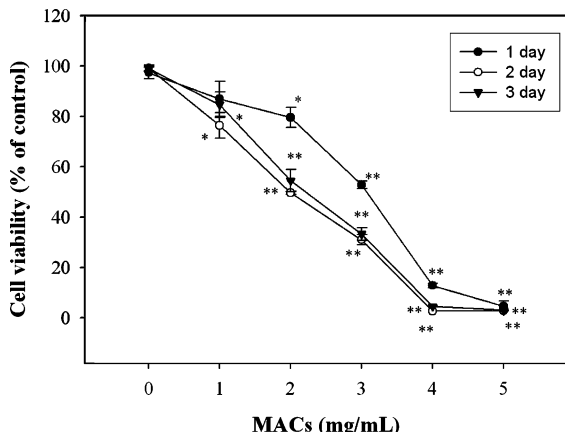


**Figure 1.** Effect of MACs on the viability of B16-F1 cells. B16-F1 cells ( $1 \times 10^5$  cells/mL) were treated with various concentrations (0–5 mg/mL) of MACs for 1 day, 2 days, and 3 days. The viability of the cells was determined by MTT assay. The survival cell number was directly proportional to formazan, which was measured spectrophotometrically at 563 nm. Values were expressed as the mean  $\pm$  SD of three independent experiments. \* $p < 0.05$  and \*\* $p < 0.001$  compared with the untreated control.

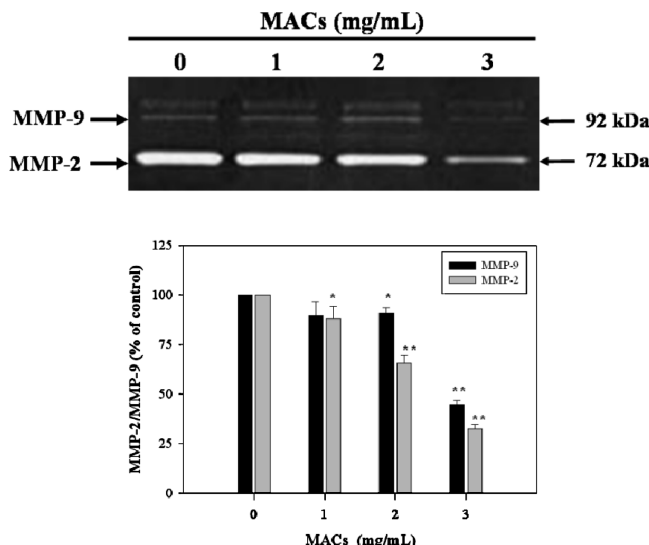


**Figure 2.** Effect of MACs on MMP-2/MMP-9 activity of B16-F1 cells. Cells were treated with various concentrations (0–3 mg/mL) of MACs for 1 day. The conditioned media were collected, and MMP-2/MMP-9 activities were determined by gelatin zymography. MMP-2/MMP-9 activities were quantified by densitometer analysis. The densitometric data were expressed as the mean  $\pm$  SD of three independent experiments. \* $p < 0.05$  and \*\* $p < 0.001$  compared with the untreated control.

**MACs Inhibit the Activation of MMP-2 and MMP-9 in B16-F1 Cells.** In many types of neoplasm, including hepatoma and lung cancer, higher levels of activated MMPs have been demonstrated in metastatic tumors and may give prognostic information independent of stage (23). Thus, tumor metastasis is highly related to the proteolytic degradation of the extracellular matrix (ECM). To further investigate, matrix-degrading proteinases are required. B16-F1 cells were treated with various concentrations of MACs for 1 day in serum-free media. At the end of the incubation, media were collected and assayed for MMP activity (gelatin zymography), as described in Materials and Methods. **Figure 2** illustrates that MMP-2 and MMP-9 activities were markedly reduced at 3 mg/mL of MACs for 1 day. Furthermore, compared with untreated cells, 3 mg/mL MACs reduced 68% and 55% of activity in MMP-2 and MMP-9, respectively.

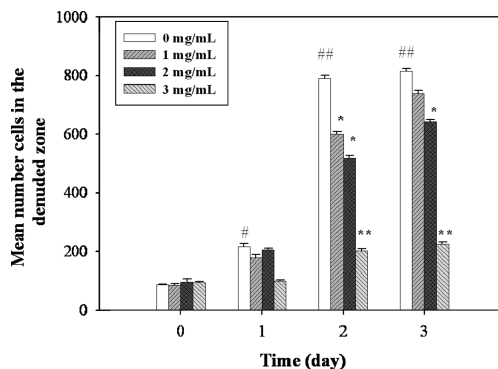


**Figure 3.** Effect of MACs on the motility of B16-F1 cells. Cell monolayers were treated with various concentrations (0–3 mg/mL) of MACs for 0, 1, 2, and 3 days. The number of cells in the denuded zone was quantitated after indicated times (0, 1, 2, and 3 days) by inverted microscopy. Quantitative assessment of the average number of the cells in the denuded zone was expressed as the mean  $\pm$  SD of three independent experiments. \* $p < 0.05$  and \*\* $p < 0.001$ , compared with the untreated control; # $p < 0.05$  and ## $p < 0.01$  compared with the 0 day-treated time.

at 1 day, respectively. The results suggested that the inhibition of MMP-2 expression by MACs might be more sensitive than MMP-9 expression and that MACs target MMP-mediated cellular events in B16-F1 cells and contribute a new mechanism for its anticancer activity. Zymographic analysis (**Figure 2**) showed that treatment with MACs at a subcytotoxic concentration at 3 mg/mL for 1 day exerted an inhibitory effect of MMP-2 and MMP-9. Therefore, MACs were able to inhibit the gelatinolysis of B16-F1 cells mediated by MMP-2 and MMP-9 in a conditioned medium. These results revealed that the anti-metastasis effect of MACs was associated with the inhibition of enzymatically degradative processes of tumor metastasis. This was the first to demonstrate the biochemical mechanism(s) by which MACs reduced the metastasis in B16-F1 cells.

**MACs Inhibits the Migration of B16-F1 Cells.** To investigate the inhibitory effect of MACs on the B16-F1 cell migration process, the wound-healing assay and Boyden chamber assay were used. In the wound-healing assay, according to a quantitative assessment, the cells were treated with various concentrations of MACs for 0, 1, 2, and 3 days. The results showed that 3 mg/mL of MACs exhibited the most effect of inhibition on cell motility after 3 days of incubation (**Figure 3**). Additionally, as compared with untreated cells, the level of B16-F1 cell number decreased 3-fold with the treatment of 3 mg/mL MACs for 3 days. These results revealed that MACs significantly inhibited the motility of B16-F1 cells.

One important characteristic of metastasis is the migratory ability of tumor cells. We used the Boyden chamber assay to quantify the migratory potential of B16-F1 cells. The results showed that MACs induced the decrease in migration of B16-F1 cells in a dose-dependent manner (**Figure 4A**). The migratory cells were markedly reduced after a 3 mg/mL MACs treatment (**Figure 4B**). It revealed that MACs significantly inhibited the migration of B16-F1 cells.

**Inhibitory Effect of MACs in Ras/PI3K-Akt Signaling.** As we have shown that treatment of MACs to B16-F1 cells inhibited the cell migration and activities of MMP-2 and MMP-9, the underlying mechanisms were further investigated as to which pathway is involved in the MACs reduced metastasis in B16-F1 cells. Therefore, the phosphorylation levels of ERK1/2 and Akt, and the protein levels of Ras, PI3K, NF- $\kappa$ B, Rho A, and Rho B after 1 day treatment with MACs (0, 1, 2, and 3 mg/mL) were analyzed. **Figure 5**

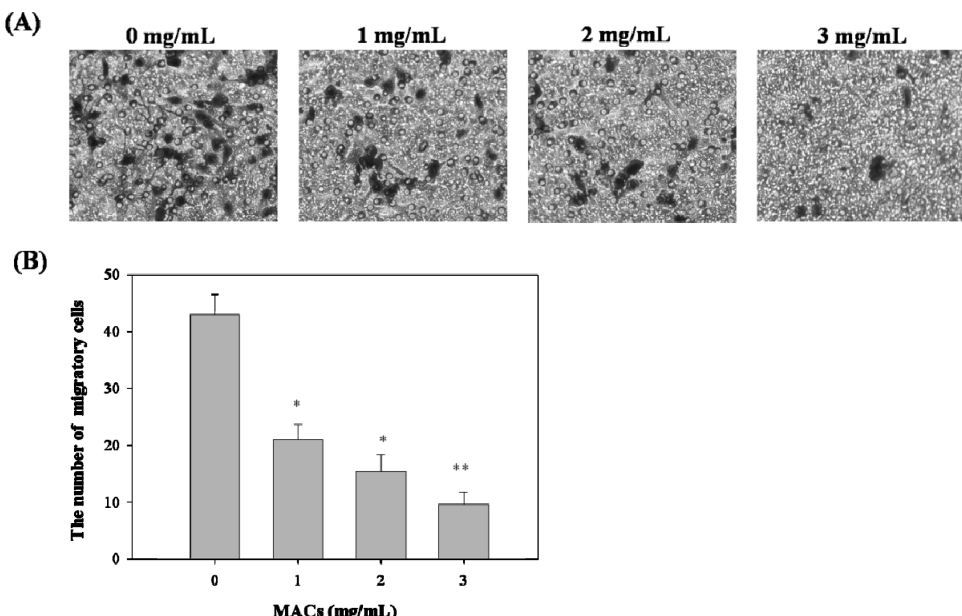


**Figure 4.** Effect of MACs on migration of B16-F1 cells. B16-F1 cells were treated with various concentrations (0–3 mg/mL) of MACs for 1 day. Cell migration was measured by Boyden chamber for 5 h with polycarbonate filters (pore size, 8  $\mu\text{m}$ ). Migration ability of B16-F1 cells were quantified by counting the number of cells that invaded the underside of the porous polycarbonate membrane under microscopy and represents the average of three experiments  $\pm$  SD. \* $p < 0.05$  and \*\* $p < 0.001$  compared with the untreated control.

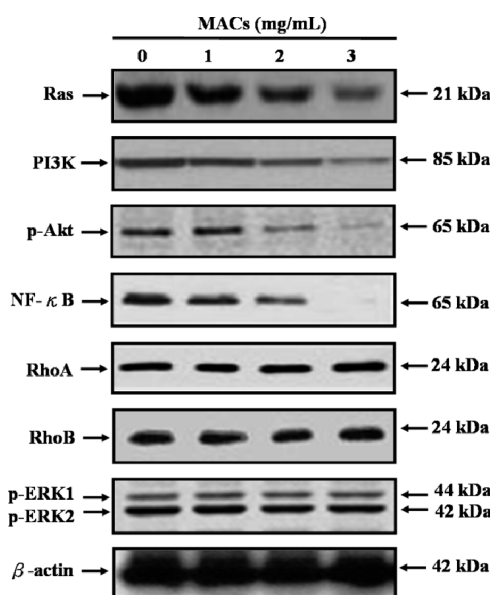


**Figure 5.** Effect of MACs on migration-related proteins of B16-F1 cells. B16-F1 cells were treated with various concentrations (0–3 mg/mL) of MACs for 1 day. Total cell lysates were prepared, and the protein expression levels of Ras, PI3K, NF- $\kappa$ B, Rho A, Rho B, and phosphorylated forms of Akt and ERK were assessed by Western blotting assay.  $\beta$ -Actin was used as a loading control. Results from three repeated and separated experiments were similar.

showed that MACs significantly suppressed the activation of Akt by decreasing the phosphorylation of Akt. In contrast, MACs did not significantly affect phospho-ERK1/2. Moreover, no significant change in the total amount of Akt and ERK1/2 proteins was observed (data not shown). In addition, MACs inhibited the protein levels of Ras, PI3K, and NF- $\kappa$ B. Whereas it did not affect the protein levels of Rho A and Rho B. Data findings revealed that the treatment of MACs diminish the activities of MMP-2 and MMP-9 in the culture media and could possibly involve a suppression of the phosphorylation of Akt.

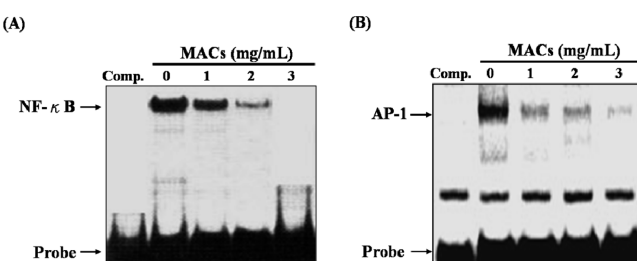


**Figure 6.** Effect of MACs on DNA binding activity of NF- $\kappa$ B and AP-1. B16-F1 cells were treated with various concentrations (0–3 mg/mL) of MACs for 1 day. Cell nuclear extracts were prepared and analyzed for (A) NF- $\kappa$ B and (B) AP-1 DNA binding activity using biotin-labeled consensus NF- $\kappa$ B and AP-1 specific oligonucleotide, then EMSA assay was performed as described in Materials and Methods. Lane 1: nuclear extracts incubated with 100-fold excess unlabeled consensus oligonucleotide (comp.) to confirm the specificity of binding. The position of NF- $\kappa$ B and AP-1 complex and free oligonucleotide are indicated. Results from three repeated and separated experiments were similar.

**MACs Inhibits DNA Binding Activity of NF- $\kappa$ B and AP-1 in B16-F1 Cells.** Transcriptional factors (for example, NF- $\kappa$ B, and AP-1) have been known to translocate into the nucleus and regulate the expression of multiple genes involved in MMPs secretion. To further explore the DNA binding activities of NF- $\kappa$ B and AP-1, the amounts of NF- $\kappa$ B and AP-1 in the cell nuclear extracts were measured by EMSA to analyze the possible inhibitory effect of MACs on DNA binding activities of NF- $\kappa$ B and AP-1. As explained in **Figure 6A,B**, NF- $\kappa$ B and AP-1 DNA binding activities were shown to be strongly inhibited by a treatment with 3 mg/mL MACs.

**Antimetastatic Effects of MACs *in Vivo*.** To further verify the antimetastatic effect of MACs *in vivo*, a B16-F1-bearing C57BL/6 mice model, which may acquire spontaneous lung and liver metastasis, was used for the studies. When mice were treated with B16-F1 cells alone (group C), all the tumor-bearing mice died after 3 weeks as shown in **Figure 7A,B**. In the B16-F1 tumor model mice, mice were treated with MACs at various

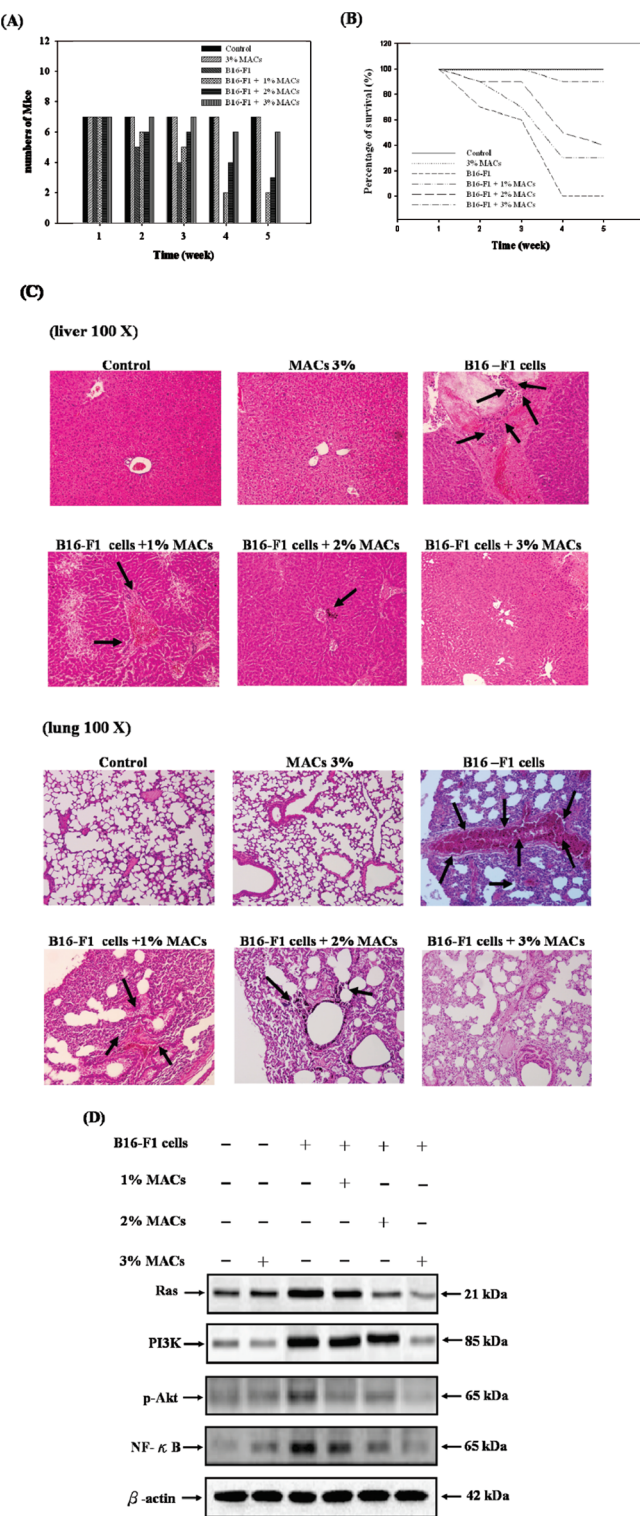


**Figure 7.** Antimetastasis effects of MACs *in vivo*. After right groinal implantation of B16-F1 cells, C57BL/6 mice were treated with MACs as described in Materials and Methods. **(A)** The number of mice. **(B)** The percentage of survival. **(C)** The tissue sections of livers and lungs of MAC-treated C57BL/6 mice determined by H&E stain and observed under an optic microscope. The black arrow indicates the metastatic nodules. All images were originally magnified 100×. **(D)** The effect of MACs on the expression levels of various proteins were assessed by immunoblot analysis.

concentrations (1%, 2%, and 3%) and were effective against tumor metastasis. Furthermore, tumor metastasis inhibition was most evident in mice treated with MACs at 3%, and mice were

alive for 5 weeks. At the end of 5 weeks, the mice were euthanized, and tissue sections of lungs and livers were observed by H&E stain. Liver and lung metastasis of mice treated with higher concentration of MACs had decreased compared with that of B16-F1 cells alone (**Figure 7C**). No sign of metastasis, as judged by parallel monitoring of the number of mice, the percentage of survival and tissue sections of livers and lungs, was observed in MACs-treated mice. The results suggested that the metastatic inhibition of higher concentration of MACs on liver might be more obvious than that in the lung. Besides, melanoma cells were the only growth at the right groin, whereas it did not cause tumor metastasis by immunohistochemistry stain (data not shown).

To further explore the antimetastatic mechanism, the amount of Ras, PI3K, Akt, and NF- $\kappa$ B in the liver were measured by Western blotting to analyze the possible inhibitory effect of MACs. As explained in **Figure 7D**, mice were treated with B16-F1 cells alone (group C) and resulted in an increase in expression levels of Ras, PI3K, Akt, and NF- $\kappa$ B. After 5 weeks, the effect of MACs in the expression levels of Ras, PI3K, Akt, and NF- $\kappa$ B were dose-dependent (groups D–F). Especially, treatment of 3% MACs could reduce the expression levels of migration-related protein, which was almost equal to the control group without any apparent signs of toxicity as evidenced by survival monitoring throughout the experiment.

## DISCUSSION

Many studies have demonstrated that anthocyanins, natural pigments from various plants, flowers, and fruits, exert anti-carcinogenic and antiproliferative effects, and are able to reduce deleterious effects of reactive oxygen species (24). Therefore, anthocyanins were regarded as chemopreventive agents. Recently, antimetastasis agents have been defined as a new class of cancer chemopreventive agent, and several studies have demonstrated that cyanidin and pelargonidin, natural products derived from blackberry or strawberry, exhibited chemopreventive and chemotherapeutic activity (25–27). The finding of the present study showed MACs have strong anticancer effects by inhibiting the metastasis ability of B16-F1 cells, and thus, it might represent a new strategy for cancer chemoprevention.

Malignant tumors invade normal tissue, involving three independent processes: the degradation of the extracellular matrix (ECM), cell metastasis, and proliferation. Metastasis has been found to be accompanied by various physiological alterations involved in the degradation of ECM, such as the overexpression of proteolytic enzyme activity, such as matrix metalloproteinases (for example, MMP-2 and MMP-9), as well as the migration and invasion of tumor cells into the bloodstream or lymphatic system to spread to another tissue or organ (28). Our study demonstrated that treatment with MACs at a noncytotoxic concentration below 3 mg/mL for 1 day exerted an inhibitory effect in a dose-dependent manner, on the highly metastatic B16-F1 cells (**Figure 2A,B**). MMP-2 and MMP-9 expressions have been linked to various cellular and physiological processes, such as cell motility, adhesion, proliferation, activation, differentiation, development, invasion, metastasis, and wound healing, most of which are also known to be modulated by MMPs. Thus, the expressions of MMP-2 and MMP-9 have been shown to play a critical role in degrading the basement membrane in the metastasis of tumor cells. One important characteristic of metastasis is the migratory ability of tumor cells. We used the wound-healing assay and Boyden chamber assay to quantify the migratory potential of B16-F1 cells. The results showed that MACs induced a dose- and time-dependent decrease

in migration with increasing concentration of MACs (**Figures 3 and 4**). The results demonstrated that MACs significantly inhibited the migration of B16-F1 cells.

Several reports have demonstrated that exposure to UV light is an inducer of gene mutation in sporadic melanoma (5). Sequentially, NF- $\kappa$ B is upregulated, leading to the deregulation of gene transcription. Metastatic melanoma mechanisms that promote constitutive activation of NF- $\kappa$ B that may occur via a down-regulation of G protein coupled receptor interacting proteins (GIP), and Ras is commonly reported in relation to melanoma progression (29). In this article, we have demonstrated that treatment of MACs inhibited the levels of Ras, PI3K, NF- $\kappa$ B, and phosphorylated Akt, whereas it has been shown that the protein levels of Rho A, Rho B, and phosphorylated ERK is unaffected (**Figure 5**). Although the signaling pathways that lead to the induction of MMP expressions are still unclear, our study reveals that MACs do not only inhibit Akt activation but also cause concurrent reductions of NF- $\kappa$ B and AP-1 DNA binding activities in B16-F1 cells (**Figure 6A,B**). Thus, our findings suggest that MACs markedly inhibited MMP-2 and MMP-9 expressions and that they may be involved in the inactivation of Akt mediated NF- $\kappa$ B signaling pathways; such an inhibitory effect on proteinase expression may contribute to the capability of MACs to inhibit cell metastasis.

Finally, using B16-F1-bearing mice, a well established animal model for metastasis (30), we found that MACs could reduce both the tumor growth and metastasis (livers and lungs) ability of B16-F1-bearing C57BL/6 mice (**Figure 7**). However, it was suggested that MACs may have an inhibitory potential for the cell metastasis of B16-F1 cells *in vivo* without showing any apparent sign of toxicity, as demonstrated by the MTT assay, the number of mice, and the percentage of survival profile. In the future, the effects of MACs on the metastasis of B16-F1 cells *in vivo* will be examined further. Moreover, recent studies have shown that the inhibitory effects of two mulberry anthocyanins, cyanidin 3-glucoside and cyanidin 3-rutinoside, on the invasion and motility of human lung carcinoma cell line were related to the inhibition of uPA and MMP-2 activities through NF- $\kappa$ B and AP-1 pathways (25). The present study first has shown that treatment of MACs inhibited the levels of Ras, PI3K, NF- $\kappa$ B, and phosphorylated Akt *in vitro*. Most notably, the current study contributes to metastasis, which was induced through the activation of Ras/PI3K/Akt and NF- $\kappa$ B, which seemed to play a central role in regulating the expression of MMP-2 and MMP-9, and MACs have also been demonstrated to be able to suppress the metastasis of B16-F1.

In conclusion, in the present study, we demonstrated the therapeutic potential of MACs for controlling tumor metastasis based on the observation of its inhibitory effect on the motility of melanoma cancer cell line B16-F1. Characterization of the detailed mechanism of the inhibitory effects of MACs showed that they inhibit B16-F1 cells, may be involved in the Ras/PI3K/Akt signaling pathway, exert inhibitory effects on NF- $\kappa$ B transcriptional factor, decrease DNA binding activity of NF- $\kappa$ B to the NF- $\kappa$ B response element, afterward decrease MMP-2 and MMP-9 activities, and then exert antimetastasis in the *in vitro* and *in vivo* models. Our results show that MACs could suppress melanoma metastasis and may act as a potential candidate for cancer chemoprevention.

## ABBREVIATIONS USED

MACs, mulberry anthocyanins; MMPs, matrix metalloproteinases; ECM, extracellular matrix; ERK, extracellular signal-regulating kinase; PI3K, phosphoinositide 3-kinase; PTEN,

phosphatase and tensin homologue deleted on chromosome 10; NF- $\kappa$ B, nuclear factor kappa B; I $\kappa$ B, inhibitor of NF- $\kappa$ B; Rho A, Ras-homologous A; Rho B, Ras-homologous B; H&E stain, hematoxylin-eosin stain.

## LITERATURE CITED

- Kang, T. H.; Hur, J. Y.; Kim, H. B.; Ryu, J. H.; Kim, S. Y. Neuroprotective effects of the cyanidin-3-O- $\beta$ -D-glucopyranoside isolated from mulberry fruit against cerebral ischemia. *Neurosci. Lett.* **2006**, *391*, 168–172.
- Koide, T.; Hashimoto, Y.; Kamei, H.; Kojima, T.; Hasegawa, M.; Terabe, K. Antitumor effect of anthocyanin fractions extracted from red soybeans and red beans *in vitro* and *in vivo*. *Cancer Biother. Radiopharm.* **1997**, *12*, 277–280.
- Kahkonen, M. P.; Heinonen, M. Antioxidant activity of anthocyanins and their aglycons. *J. Agric. Food Chem.* **2003**, *51*, 628–633.
- Hurst, E. A.; Harbour, J. W.; Cornelius, L. A. Ocular melanoma: a review and the relationship to cutaneous melanoma. *Arch. Dermatol.* **2003**, *139*, 1067–1073.
- Bauer, J.; Garbe, C. Acquired melanocytic nevi as risk factor for melanoma development. A comprehensive review of epidemiological data. *Pigment Cell Res.* **2003**, *16*, 297–306.
- Gilchrest, B. A.; Eller, M. S.; Geller, A. C.; Yaar, M. The pathogenesis of melanoma induced by ultraviolet radiation. *N. Engl. J. Med.* **1999**, *340*, 1341–1348.
- Emmert-Buck, M. R.; Roth, M. J.; Zhuang, Z.; Campo, E.; Rozhin, J.; Sloane, B. F.; Liotta, L. A.; Stetler-Stevenson, W. G. Increased gelatinase A (MMP-2) and cathepsin B activity in invasive tumor regions of human colon cancer samples. *Am. J. Pathol.* **1994**, *145*, 1285–1290.
- Herbst, R. S.; Yano, S.; Kuniyasu, H.; Khuri, F. R.; Bucana, C. D.; Guo, F.; Liu, D.; Kemp, B.; Lee, J. J.; Hong, W. K.; Fidler, I. J. Differential expression of E-cadherin and type IV collagenase genes predicts outcome in patients with stage I non-small cell lung carcinoma. *Clin. Cancer Res.* **2000**, *6*, 790–797.
- Yang, S. A.; Paek, S. H.; Kozukue, N.; Lee, K. R.; Kim, J. A. Alpha-chaconine, a potato glycoalkaloid, induces apoptosis of HT-29 human colon cancer cells through caspase-3 activation and inhibition of ERK 1/2 phosphorylation. *Food Chem. Toxicol.* **2006**, *44*, 839–846.
- Kaomongkolgit, R.; Cheepsunthorn, P.; Pavasant, P.; Sanchavananakit, N. Iron increases MMP-9 expression through activation of AP-1 via ERK/Akt pathway in human head and neck squamous carcinoma cells. *Oral Oncol.* **2008**, *44*, 587–594.
- Ye, M.; Hu, D.; Tu, L.; Zhou, X.; Lu, F.; Wen, B.; Wu, W.; Lin, Y.; Zhou, Z.; Qu, J. Involvement of PI3K/Akt signaling pathway in hepatocyte growth factor-induced migration of uveal melanoma cells. *Invest. Ophthalmol. Vis. Sci.* **2008**, *49*, 497–504.
- Hennessy, B. T.; Smith, D. L.; Ram, P. T.; Lu, Y.; Mills, G. B. Exploiting the PI3K/AKT pathway for cancer drug discovery. *Nat. Rev. Drug Discovery* **2005**, *4*, 988–1004.
- Yoon, S. O.; Shin, S.; Lee, H. J.; Chun, H. K.; Chung, A. S. Isoginkgetin inhibits tumor cell invasion by regulating phosphatidylinositol 3-kinase/Akt-dependent matrix metalloproteinase-9 expression. *Mol. Cancer Ther.* **2006**, *5*, 2666–2675.
- Chung, T. W.; Lee, Y. C.; Kim, C. H. Hepatitis B viral HBx induces matrix metalloproteinase-9 gene expression through activation of ERK and PI-3K/AKT pathways: involvement of invasive potential. *FASEB J.* **2004**, *18*, 1123–1125.
- Lee, S. O.; Jeong, Y. J.; Im, H. G.; Kim, C. H.; Chang, Y. C.; Lee, I. S. Silibinin suppresses PMA-induced MMP-9 expression by blocking the AP-1 activation via MAPK signaling pathways in MCF-7 human breast carcinoma cells. *Biochem. Biophys. Res. Commun.* **2007**, *354*, 165–171.
- Fritz, G.; Kaina, B. Rho GTPases: promising cellular targets for novel anticancer drugs. *Curr. Cancer Drug Targets* **2006**, *6*, 1–14.
- Khosravi-Far, R.; Solski, P. A.; Clark, G. J.; Kinch, M. S.; Der, C. J. Activation of Rac1, RhoA, and mitogen-activated protein

- kinases is required for Ras transformation. *Mol. Cell. Biol.* **1995**, *15*, 6443–6453.
- (18) Chen, Z.; Sun, J.; Pradines, A.; Favre, G.; Adnane, J.; Sebti, S. M. Both farnesylated and geranylgeranylated RhoB inhibit malignant transformation and suppress human tumor growth in nude mice. *J. Biol. Chem.* **2000**, *275*, 17974–17978.
- (19) Liu, L. K.; Lee, H. J.; Shih, Y. W.; Chyau, C. C.; Wang, C. J. Mulberry anthocyanin extracts inhibit LDL oxidation and macrophage-derived foam cell formation induced by oxidative LDL. *J. Food Sci.* [online early access]. DOI: 10.1111/j.1750-3841.2008.00801.x. Published Online: Jun 5, **2008**.
- (20) Fuleki, T.; Francis, F. J. Quantitative methods for anthocyanins. 2. Determination of total anthocyanin and degradation index for cranberry juice. *J. Food Sci.* **1968**, *33*, 78–83.
- (21) Chu, S. C.; Chiou, H. L.; Chen, P. N.; Yang, S. F.; Hsieh, Y. S. Silibinin inhibits the invasion of human lung cancer cells via decreased productions of urokinase-plasminogen activator and matrix metalloproteinase-2. *Mol. Carcinog.* **2004**, *40*, 143–149.
- (22) Hoppe-Seyler, F.; Butz, K.; Rittmuller, C.; vonKnebel Doeberitz, M. A rapid microscale procedure for the simultaneous preparation of cytoplasmic RNA, nuclear DNA binding proteins and enzymatically active luciferase extracts. *Nucleic Acids Res.* **1991**, *19*, 5080.
- (23) Murrer, D.; Breathnach, R.; Engelman, A.; Millon, R.; Bronner, G.; Flesch, H.; Dumont, P.; Eber, M.; Abecasis, J. Expression of collagenase related metalloproteinases genes in human lung or head and neck tumors. *Int. J. Cancer.* **1991**, *48*, 550–556.
- (24) Ramirez-Tortosa, C.; Andersen, O. M.; Gardner, P. T.; Morrice, P. C.; Wood, S. G.; Duthie, S. J.; Collins, A. R.; Duthie, G. G. Anthocyanin rich extract decreases indices of lipid peroxidation and DNA damage in vitamin E-depleted rats. *Free Radical Biol. Med.* **2001**, *31*, 1033–1037.
- (25) Chen, P. N.; Chu, S. C.; Chiou, H. L.; Kuo, W. H.; Chiang, C. L.; Hsieh, Y. S. Mulberry anthocyanins, cyanidin 3-rutinoside and cyanidin 3-glucoside, exhibited an inhibitory effect on the migration and invasion of a human lung cancer cell line. *Cancer Lett.* **2006**, *235*, 248–259.
- (26) Ding, M.; Feng, R.; Wang, S. Y.; Bowman, L.; Lu, Y.; Castranova, V.; Jiang, B. H.; Shi, X. Cyanidin-3-glucoside, a natural product derived from blackberry, exhibits chemopreventive and chemotherapeutic activity. *J. Biol. Chem.* **2006**, *281*, 17359–17368.
- (27) Roy, M.; Sen, S.; Charkraborti, A. S. Action of pelargonidin on hyperglycemia and oxidative damage in diabetic rats: Implication for glycation-induced hemoglobin modification. *Life Sci.* **2008**, *82*, 1102–1110.
- (28) Kleiner, D. E.; Stettler-Stevenson, W. G. Matrix metalloproteinases and metastasis. *Cancer Chemother. Pharmacol.* **1999**, *43*, S42–S51.
- (29) Ueda, Y.; Richmond, A. NF- $\kappa$ B activation in melanoma. *Pigment Cell Res.* **2006**, *19*, 112–124.
- (30) Baniyash, M.; Smorodinsky, N. I.; Yaakubovicz, M.; Witz, I. P. Serologically detectable MHC and tumor-associated antigens on B16 melanoma variants and humoral immunity in mice bearing these tumors. *J. Immunol.* **1982**, *129*, 1318–1323.

Received for review April 27, 2008. Revised manuscript received June 20, 2008. Accepted July 29, 2008. Grant support was provided by Department of Health, Republic of China (DOH93-TD-1012) and Subsidized Project of the Chung Shan Medical University, Taichung, Taiwan (94-OM-B-018).

JF8013102